ACE2: Global Digital Elevation Model

R.G. Smith & P.A.M.Berry
EAPRS Laboratory, De Montfort University, Leicester, UK

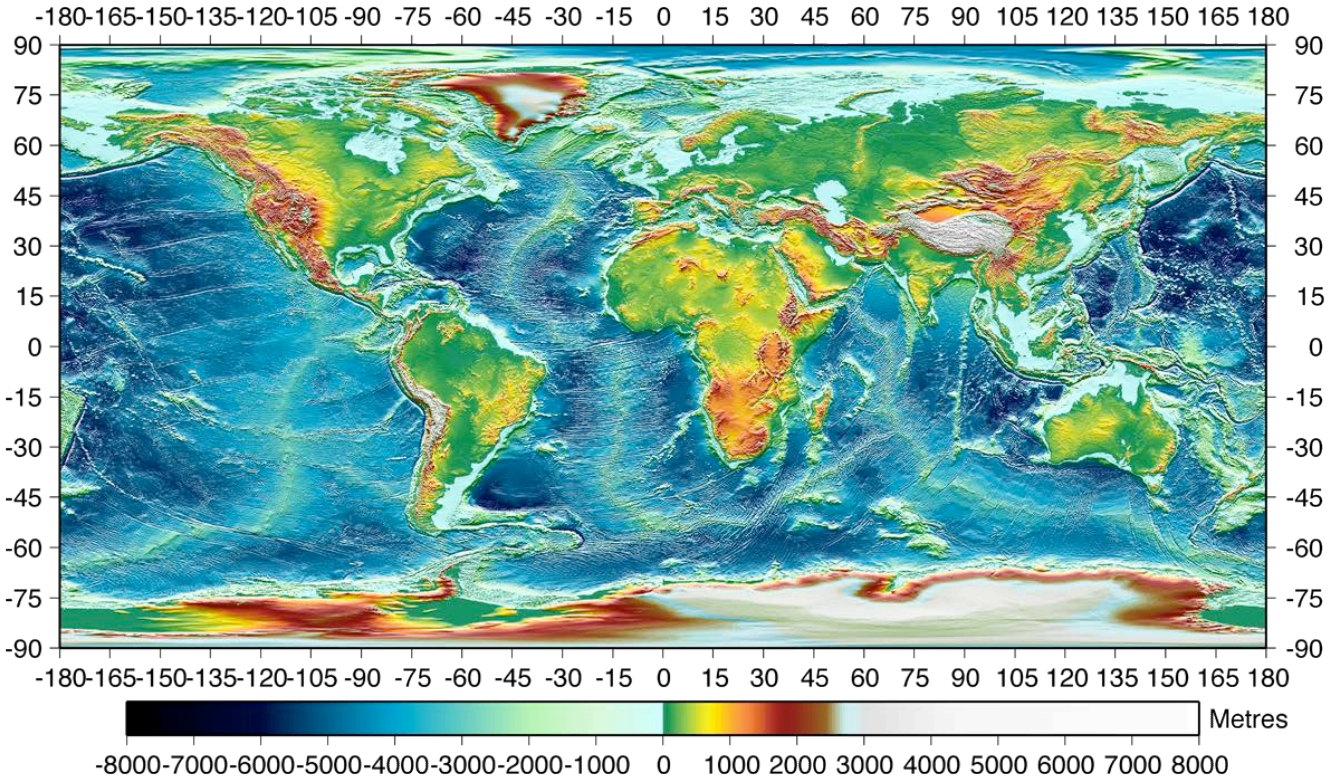

Table of Contents

List of Figures

List of Tables

ACRONYMS LIST

ACE	Altimeter Corrected Elevations
ACE2	Altimeter Corrected Elevations 2
DEM	Digital Elevation Model
DNSC	Danish National Space Center
GDR	Geophysical Data Record
GDEM	Global Digital Elevation Model
GLOBE	Global Land One-km Base Elevation Project
GTOPO30	Global Topography30
USGS	United States Geological Survey
SAR	Synthetic Aperture Radar
SGDR	Sensor Geophysical Data Record
SRTM	Shuttle Radar Topography Mission

1. Background

Detailed accurate Digital Elevation Model (DEM) data have historically not been available on other than a regional scale, and often have uncertainties in both vertical and horizontal precision. The first altimeter-informed Global Digital Elevation Model (GDEM), ACE (Altimeter Corrected Elevations) was created by fusing altimeter derived heights (produced using a system of multiple retrackers) with ground truth available from a range of publicly available datasets to create an enhanced GDEM (Berry 2000; Berry et al., 2000; Hilton et al., 2003). This represented a considerable enhancement in the quality of publically available GDEMs, because the altimeter arcs of precisely measured heights enabled the correction of many of the vertical datum errors in the various ground truth datasets that were stitched together to form GDEMs such as GTOPO30 (USGS, 1996) and GLOBE (GLOBE team, 1999).

However, this was curtailed in spatial resolution to 30” (about 1km at the equator) by the level of detail available in the ground truth, and the spatial distribution of the altimeter tracks from the ERS1 Geodetic Mission, which have an average across-track spacing of 4km and an along-track sampling of about 350m. The release of the SRTM dataset derived using interferometric SAR (Hensley et al., 2000) presents a 3” dataset up to a latitude limit of 60N and 54S. This dataset represents a very substantial improvement in the quality and spatial resolution of the publicly available DEM data, with a global vertical accuracy estimate of +/- 16m (ibid). However, as both global and regional evaluations with ground truth have shown, there are regional differences in the estimate of accuracy of this dataset (Denker, 2004; Brown et al., 2005; Hall et al., 2005; Smith & Sandwell., 2003); crucially, these quality assessments are limited by the availability of ground truth. It was therefore decided to carry out a global assessment of the SRTM dataset by reprocessing the ERS1 Geodetic Mission altimeter dataset (Capp., 2001) using an augmented version of the original expert system (Berry, 2000) to optimise the height retrieval and hence determine whether enhancements could be made to the SRTM dataset by fusion with altimeter derived heights from multiple satellite altimeters.

1. Satellite Radar Altimeter datasets

In this section, the characteristics and available data from current and past satellite altimeters are briefly reviewed.

Satellite altimeters work by directing a stream of pulses of microwave energy directly down onto the earth's surface, receiving the returned echoes, and hence calculating the range from the satellite to the underlying surface. After correcting this range for the effects of signal propagation through the Earth's atmosphere, and adding in precise orbit data to give the position of the satellite with respect to that of the Earth, the height of the earth's surface above some reference surface may be determined. This technique has been highly efficient in mapping the Earth's oceans surfaces, producing heights to a vertical position of 5 cm or better (Fu & Cazenave, 2001). However, over land surfaces, the shape of the echoes returned to the satellite can be extremely complicated. In order to retrieve an accurate range to surface from these data, it is necessary to identify that part of the returned echo which has returned from directly beneath the satellite, and separate this part out from the rest of the echo.

The key to unlocking the potential of satellite radar altimetry over land targets was the development of an expert system that characterises each waveform according to shape, and then applies one of 12 retracking algorithms to obtain the best range to surface, by identifying the nadir return (Berry, 2000; Berry et al., 2000). Over flat terrain, this identification is fairly simple; however, most of the earth's land surface has varying topography and therefore the retracking process must identify and account for slope components in order to retrieve the nadir range. These data are fused with orbit data (Scharroo & Vischer, 1998) and the EGM96 geoid model (Lemoine et al., 1998) is used to transform to orthometric heights.

A similar approach was taken to the retracking of

Table 1 Missions and Datasets used for initial ACE2 analysis

Mission	Along-track sampling rate	Mode	Gate Width	Time span used
Topex Ku Band	10Hz/594m	320Mhz	0.47m	Mar 1994-Aug 2002
ERS-1	20Hz/332m	320Mhz/80Mhz switching by mask *	0.45m/1.82m	April 1994 – March 1995
Envisat RA-2 Ku Band	18Hz/369m	320Mhz/80Mhz/20Mhz autonomous selection	0.47m/1.87m/7.5m	Aug 2002-Jul 2005
Jason-1 Ku Band	20Hz/297m	320Mhz	0.47m	Aug 2002-Mar 2004

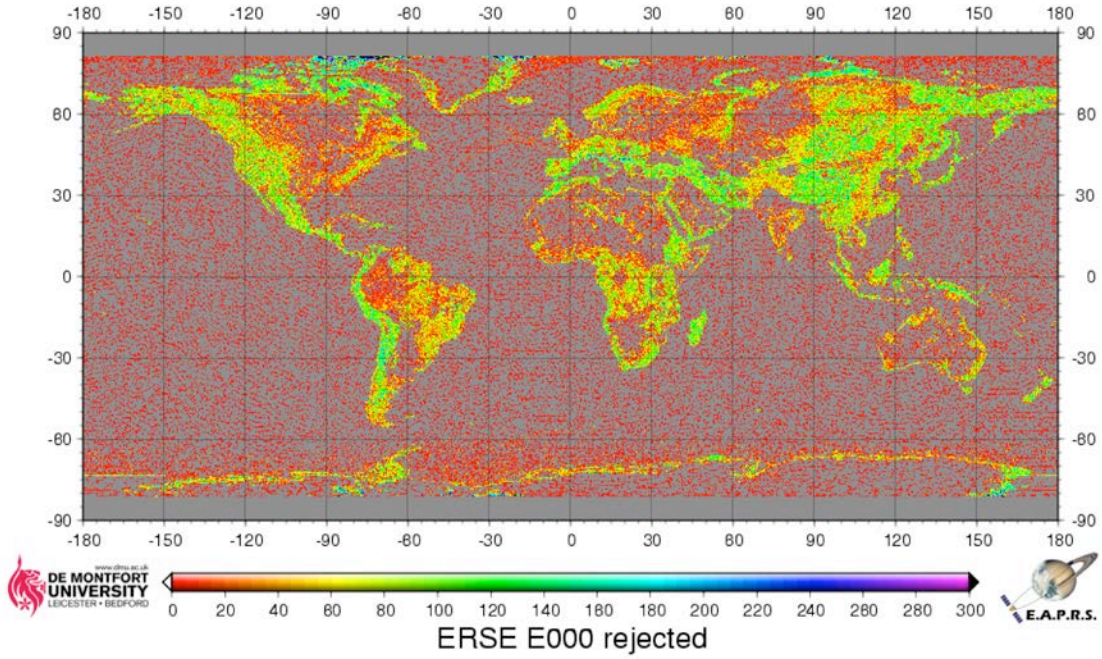

Figure 1 Rejected waveforms from ERS1 GM

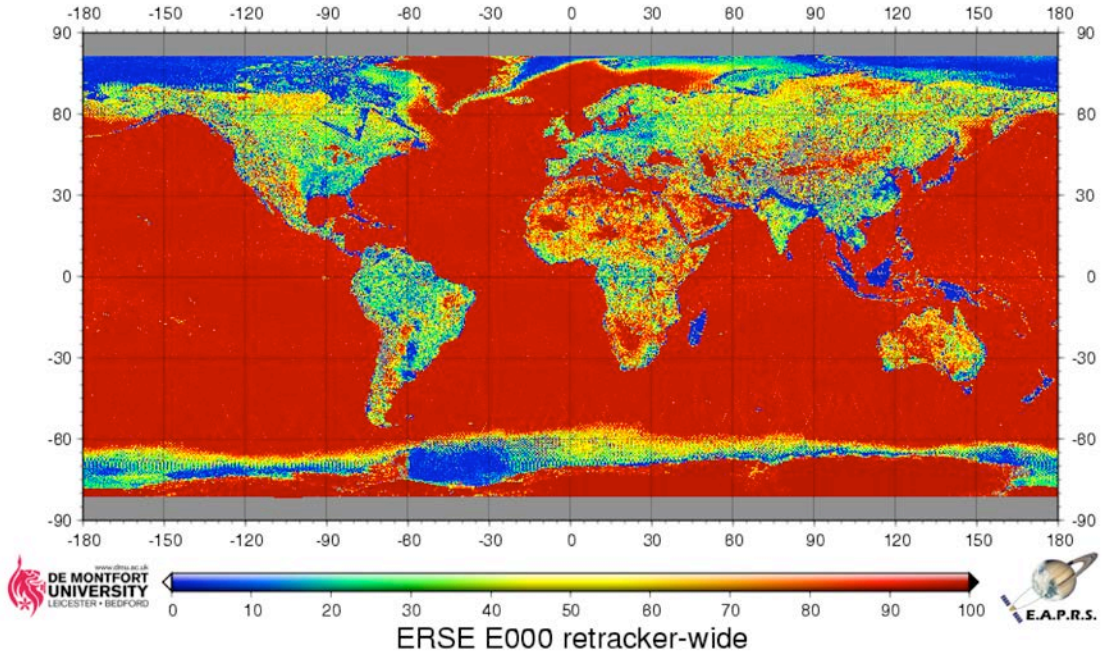

Figure 2 Wide waveforms from ERS1 GM

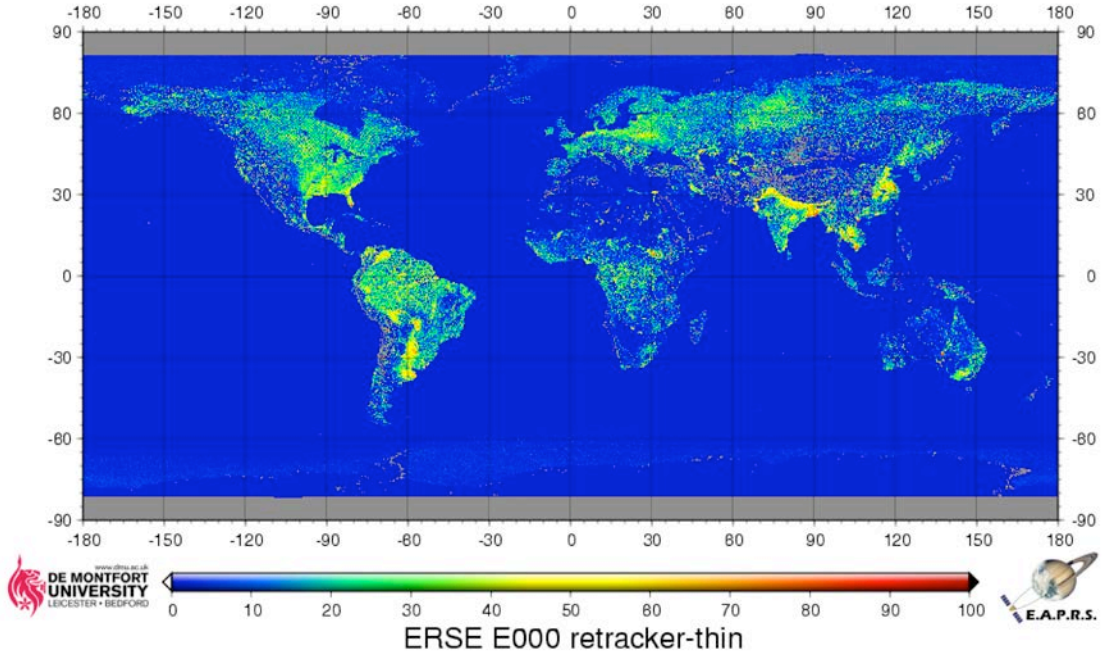

Figure 3 Narrow waveform distribution from ERS1-GM

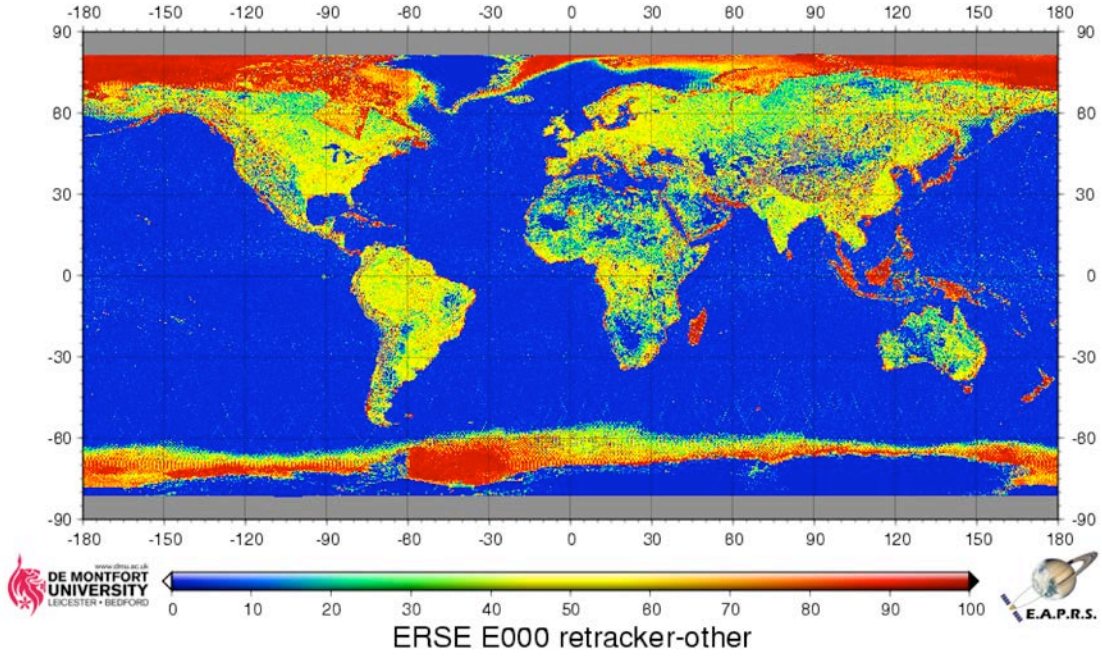

Figure 4 Complex waveform distribution from ER1-GM

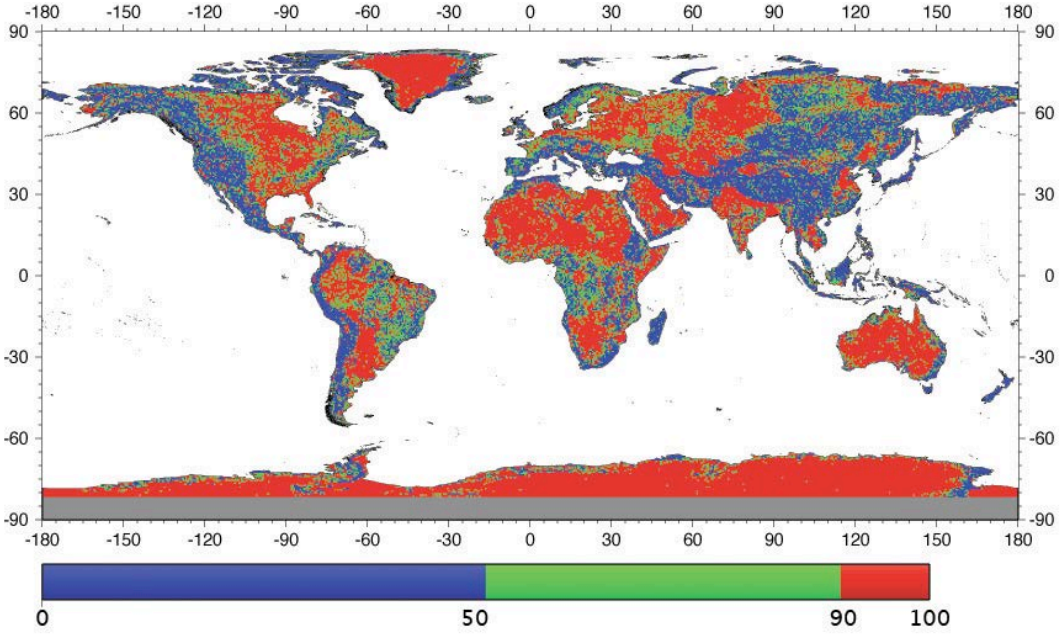

Figure 5 Banding of ERS1-GM based upon percentage obtained of theoretical maximum number of waveforms

ENVISAT RA-2 SGDR data (Benveniste et al., 2002). For TOPEX, the GDR dataset (Benada & Digby, 1997) was merged with the waveform data (Algiers et al., 1993). Again a tuned expert system was utilised to obtain optimal range to surface from each waveform. One year of Jason-1 data (Zanife et al., 2004) was also reprocessed. Statistics for the datasets are given in Table 1.

The first requirement was to assess the geographic distribution of retracked ERS-1 data. Accordingly, all waveforms from the entire Geodetic Mission were analysed, and the proportion of these data rejected was calculated (Figure 1); each waveform was then retracked, and a series of combined plots made of the global distribution of the different categories of waveform shape. The first category, derived from three of the expert system retrackers (Berry, 2000) contained wide waveforms (Figure 2) which are typically returned from desert surfaces, as is very clearly seen over Australia, or from snow. The second category, of narrow waveforms, return from wet land or inland water (Figure 3); here, the Ganges in India and the Pantanal in Argentina are clearly seen. Finally, a composite category of 'complex' waveforms' was created, as these waveforms generally return from complex topographic surfaces and sea ice (Figure 4).
All waveforms were then retracked to yield height estimates, using the EGM96 geoid model (Lemoine et al., 1998) to convert to orthometric heights. The total percentage of waveforms which could be successfully retracked was then calculated as a percentage of the theoretical maximum for each 7.5' pixel, and the results were sorted into one of three categories according to the percentage of the theoretical maximum waveform count

successfully recovered. A global statistical analysis was then performed (Berry et al., 2007). For clarity, the global banding thresholds are given in Table 2, and the global results are shown in Figure 5.

Table 2 Banding of ERS-1 GM waveform recovery

Band	Range (percent)
3	>90
2	50 - 90
1	0-50

The altimeter and SRTM datasets were then compared globally on a range of spatial and vertical scales, to obtain estimates of the precision of the SRTM heights.

2. SRTM Evaluation with Altimetry

In this section, the results of the global evaluation of the SRTM dataset with multi-mission satellite radar altimetry are briefly summarised. Figure 6 shows the first global comparison that was performed; here, the global differences are displayed banded into 16m vertical bins, to illustrate the spatial correlation that exists between many of the difference data.

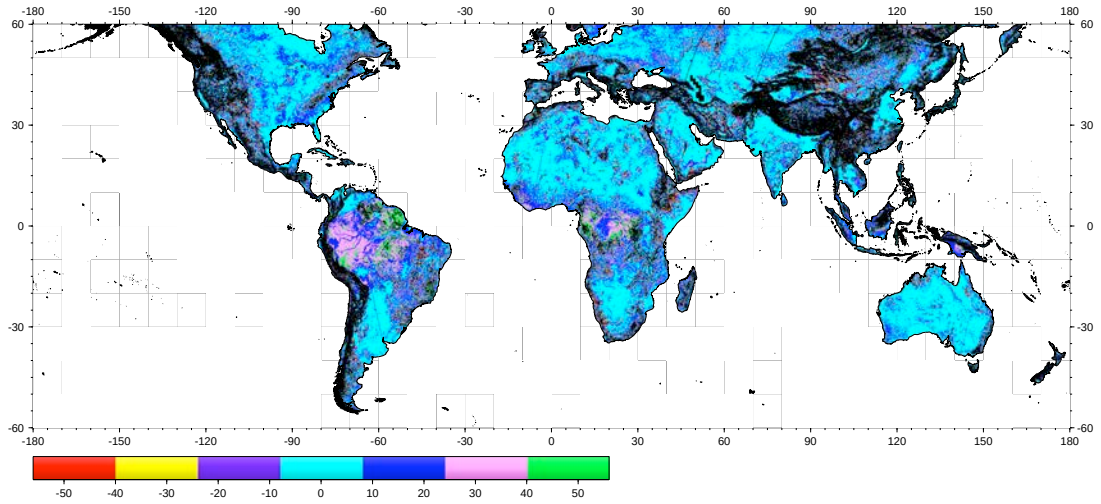

Figure 6 Global difference dataset (SRTM - altimetry) banded into 16m difference bins

Following this initial global comparison, a series of detailed into comparisons were performed, to investigate further the difference data sets. Note that in all these figures, areas where the capture of altimeter echoes was poor have been grayed out. As the comparison was judged unreliable in these regions due to the paucity of comparison data. These mountainous areas are considered later in this user guide, because the availability of data from the EnviSat RA2 has allowed detailed profiles of height differences to be analysed. The reason that this is possible is because end is that it has a third mode of

operation on its ultimate, which allows the instruments to remain in lock even over extremely rough terrain.

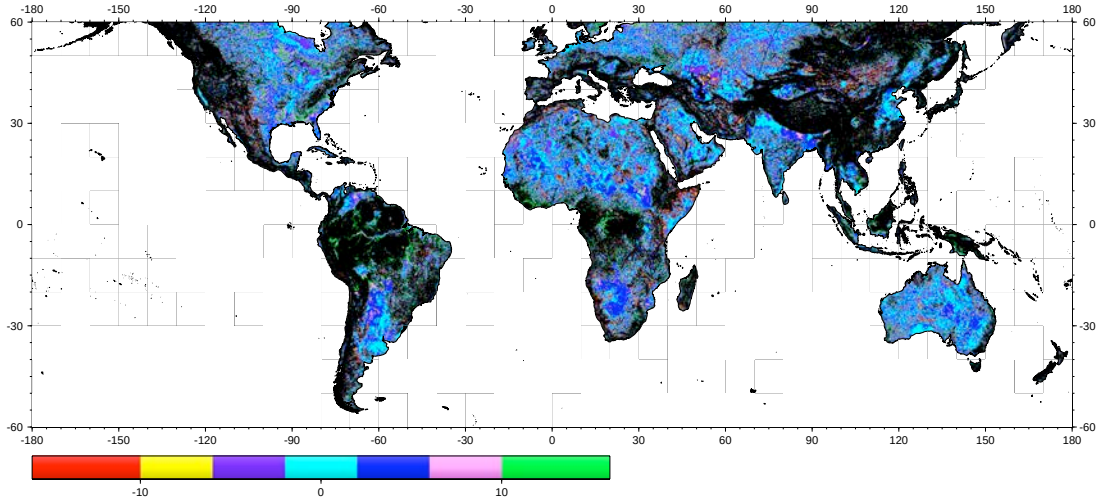

Figure 7 Global difference dataset showing where SRTM dataset is within its global stated accuracy

The first of these detailed into comparisons is shown in Figure 7, which is bandied to show all those areas where the SRTM is within its stated accuracy limit, as determined by comparison with altimeter data. As previously, areas where the altimeter was unable to capture enough data to allow a comparison to be made have been greyed out. Additionally, areas outside the accuracy limit stated for the SRTM (± 16m) have also been excluded. It is clear that, over many regions, the vertical accuracy of the SRTM dataset is actually extremely high; this is particularly so in relatively flat terrain. Over the vast majority of Australia, Northern Africa, the Kalahari Desert, and much of both North America and the southern part of South America very good agreement is seen; the same is clearly true over much of Western Europe.

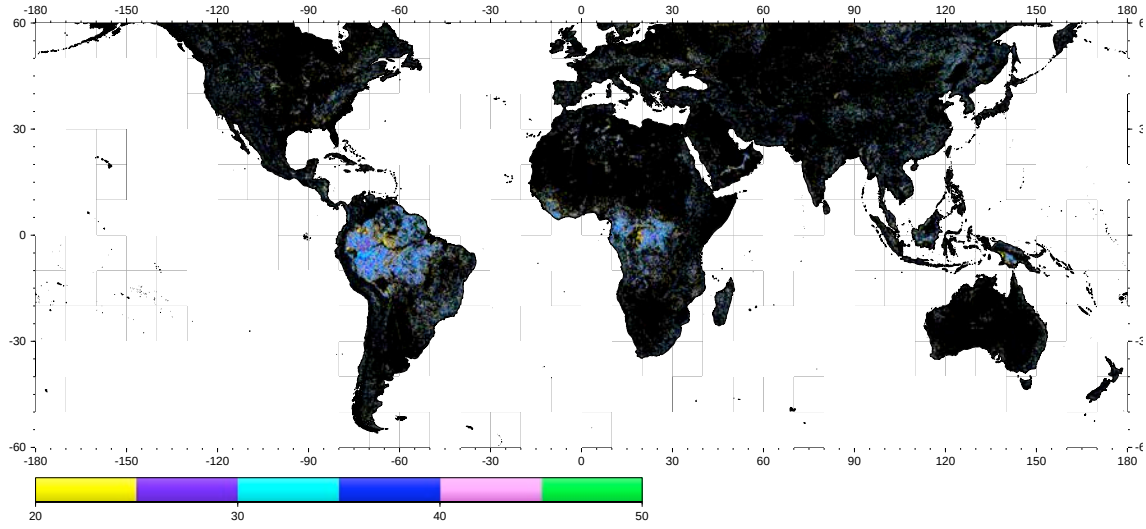

Figure 8 Global difference dataset banded to show areas of significant difference between the SRTM and the altimeetr datasets

Figure 8 shows a global comparison between these two datasets, banded to show areas where there is significant difference between them. As before, areas where the altimeter data are too sparse to permit a meaningful comparison to be made have been greyed out. The most striking features of this plot are the differences very clearly seen over the Congo and the Amazon rainforests. This is an expected outcome of the different ways that the SAR and the altimeter instruments interact with the underlying terrain. The SRTM dataset, gathered using an interferometric SAR technique, is returning the majority of its signal from somewhere within the upper canopy in dense rainforest areas (Kellndorfer et al., 2004). This was a known complication of the use of this technique for global mapping, and is the reason that the SRTM mission was flown during northern hemisphere winter (Farr, T. G., et al., 2007). In contrast, the altimeter data reflect most strongly from the underlying ground surface, and therefore they effectively penetrate through the rainforest canopy and may be used to derive ground heights.

Over these regions, it was therefore decided to utilise multi-mission satellite altimeter data, which returns from the underlying ground, to replace the SRTM pixels over rainforest areas. Beyond the SRTM latitude limits, multi-mission altimeter data would be fused with ground truth to generate the best topographic surface.

3. Data Fusion

For all areas categorised as Band 3, the ERS1 Geodetic Mission heights were used to warp the SRTM pixels according to a complex protocol. As an illustration, the results for changes within the SRTM stated accuracy are given in Table 1. Clearly, these small vertical changes are made in primarily flat areas. Those regions with larger geographically correlated differences due to rainforest cover (ibid)) have been identified and replaced with an altimeter derived Digital Elevation Model. To illustrate the effectiveness of radar altimetry in penetrating to the underlying ground surface, Figure 9 shows an area of the Amazon rainforest where the tree cover ranges from continuous to non-existent. For comparison purposes, Figure 10 shows a Google map of the same area; here, the areas of deforestation are very clearly seen, and comparison of Figures 9 and 10 shows the almost perfect correlation between the difference data in Figure 9 and the deforested areas in Figure 10. This approach has also allowed enhanced retrieval of the River Heights in the region; whilst, over the major tributary is within the Amazon basin, the SRTM heights are reasonably correct, over the smaller tributaries and particularly in areas of rougher terrain, the surrounding tree canopy has contaminated the heights determined by the interferometric SAR technique. By replacing these data with an accurate DEM derived from multi-mission satellite radar altimetry, the river network is much more correctly delineated.

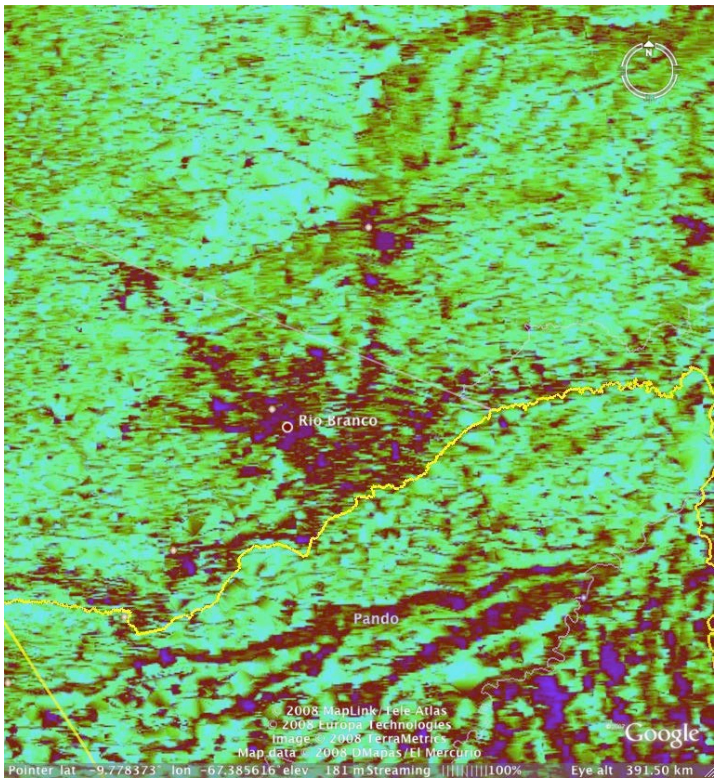

Figure 9 Rio Branco and surrounding area showing differences between the multi-mission satellite radar altimeter heights and the SRTM

Figure 10 Rio Branco area as depicted by Google Earth

A small number of other regions have been found where sustained differences exist, primarily over desert dune fields (ibid). An example of these differences is given in Figure 11. It is clear that correlated areas of difference exist; these are attributed to the different ways in which the two instruments perceived dune fields. Here, the two data sets have been fused, retaining the high-frequency information held by the SRTM dataset whilst correcting the offsets detected by the satellite radar altimeter.

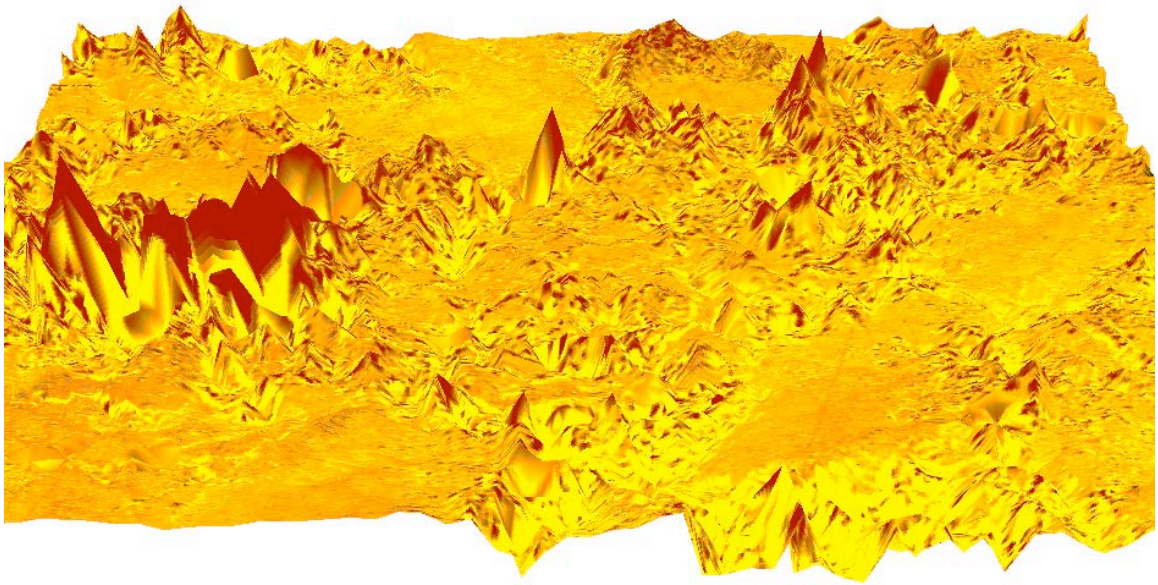

Figure 11 3D representation of the difference dataset over part of the Sahara desert

Having identified and investigated these areas of sustained difference between the two data sets, the global protocols were finally defined and implemented.
For areas classed as Band 2, all pixels with good altimeter values have been assessed, and where sufficient altimeter data exist, sustained vertical differences from the SRTM heights have been resolved by fusing the two datasets. The statistics obtained are given in Figure 12.

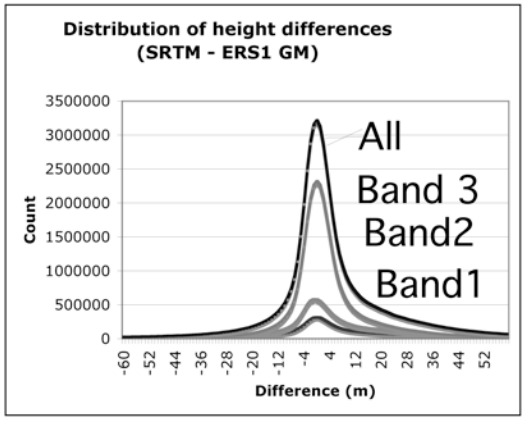

Figure 12 Height differences sorted according to banding of ERS1-GM data

A range of additional techniques was also utilised, To enhance the SRTM dataset in different regions. The methodology included examining profiles of EnviSat RA-2 data over rougher terrain. These arcs of ultimate height data were effectively used as geodetic control arcs and were used to remove height errors within the SRTM DEM. Finally, over mountainous terrain (primarily the Himalayas) where the topography is so extreme that no altimeter mission has succeeded in maintaining lock, the SRTM data have been retained.

For regions outside the latitude bounds of the SRTM, all available altimeter data were fused with a range of existing ground truth to create the best possible topographic representation and extend the DEM to a full global model.

4. ACE2 auxiliary datasets

Clearly, this complex analysis and fusion process has generated a wealth of information relevant for users of ACE2. In order to ensure that users will be fully informed, it was decided to issue three additional matrices along with the actual height dataset. The first, a source matrix, summarises the source information for every pixel (Figure 12). This is similar to the approach taken in the generation of prior GDEMs.

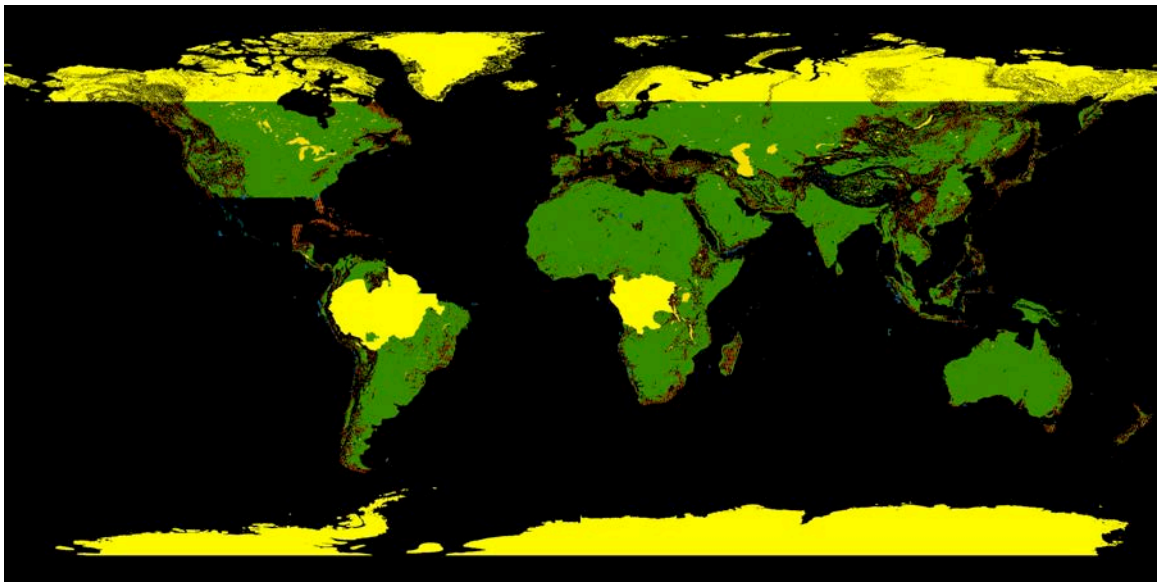

Figure 12 Global source matrix for ACE2

Table 3 gives the key to Figure 12, explaining the different source codes used.

Table 3 Source matrix definitions

Matrix number	Source
0	Pure SRTM (above 60°N pure GLOBE data, below 60S pure ACE [original] data)
1	SRTM voids filled by interpolation and/or altimeter data
2	SRTM data warped using the ERS-1 Geodetic Mission
3	SRTM data warped using EnviSat & ERS-2 data
4	Mean lake level data derived from Altimetry
5	GLOBE/ACE data warped using combined altimetry (only above 60°N)
6	Pure altimetry data (derived from ERS-1 Geodetic Mission, ERS-2 and EnviSat data using Delaunay Triangulation and Bilinear interpolation

Secondly, a quality matrix gives an assessment of the height accuracy (Figure 13). This is quite variable, and it depends on the extent to which the altimeter datasets have been able to assess the SRTM dataset. For all areas where sufficient altimeter data exists to allow an accurate assessment of the heights included in the ACE2 DEM, this accuracy assessment has been passed through to the quality matrix. Over very mountainous regions, where very little altimeter data exists, the stated global accuracy of the SRTM dataset has been utilised. The code identifiers for the quality matrix are given in table 4.

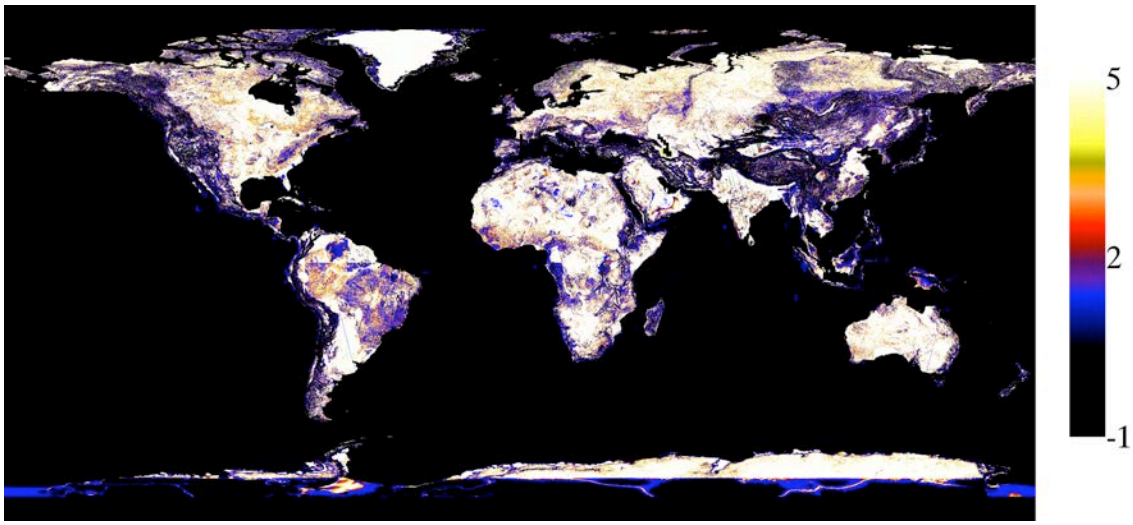

Figure 13 Global quality matrix for ACE2

Table 4 Quality Matrix definitions

Matrix number	Quality
0	Generic – use base datasets
1	Accuracy of greater than ±16m
2	Accuracy between ±16m - ±10m
3	Accuracy between ±10m - ±5m
4	Accuracy between ±5m - ±1m
5	Accuracy between ±1m

Finally, and critically, a confidence matrix is included, to give feedback on the certainty with which the error estimate has been made, again reflecting the variable extent to which independent confirmation of the height values has been obtained. This matrix contains information for every pixel of the ACE2 GDEM, and it is recommended that this matrix always be examined in conjunction with the accuracy matrix, in order to make informed judgements about the suitability of the ACE2 GDEM for a particular application. The codes for the confidence matrix are given in Table 5.

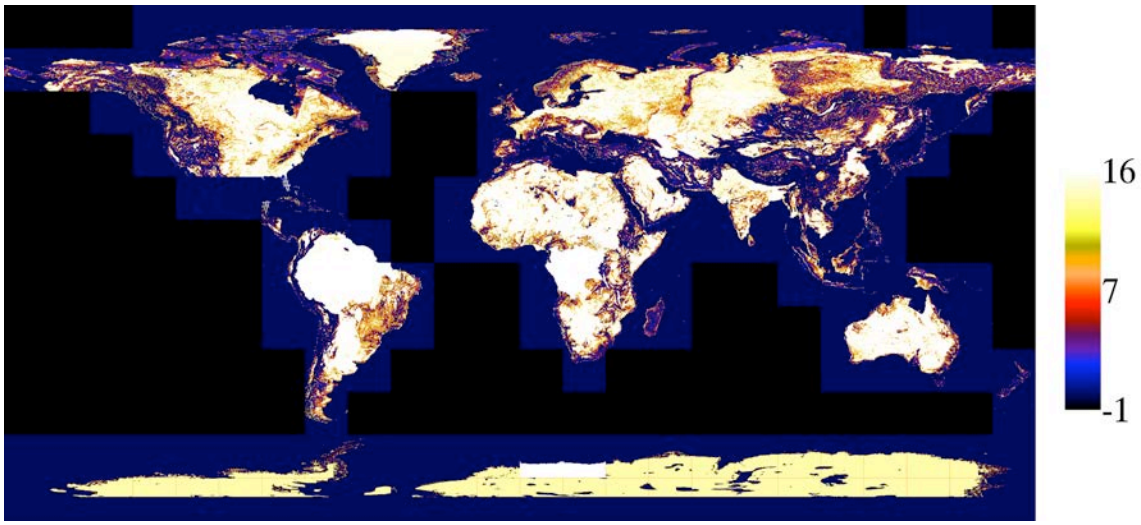

Figure 14 Confidence matrix for ACE2

Table 5 Confidence Matrix definitions

Matrix Number	Confidence rating
0	No confidence could be derived due to lack of data
1	Heights generated by interpolation
2	Low confidence
3	Low confidence
4	Low confidence
5	Medium confidence
6	Medium confidence
7	Medium confidence
8	Medium confidence
9	Medium confidence
10	Medium confidence
11	Medium confidence
12	Medium confidence
13	High confidence
14	High confidence
15	High confidence
16	High confidence
17	Inland water confidence
18	Inland water confidence
19	Inland water confidence
20	Inland water confidence
21	Inland water confidence

The ACE2 dataset is available at a range of spatial resolutions; 3", 9", 30" and 5'. The dataset may be freely downloaded from the ACE2 website (http://tethys.eaprs.cse.dmu.ac.uk/ACE2); the only requirement is that users register.

For the lowest spatial resolution models, the dataset may be downloaded in its entirety; alternatively, individual 15° X 15° titles can be selected. This approach has been taken to minimise the amount of data that users are required to download in one go. The detailed format information is contained in a README file which is downloaded together with the dataset. For completeness, this README file is included in the Userguide as Appendix A.

Additionally, two models have been developed which contain a fusion of the ACE2 data with mean seasurface heights (Figure 15) and with bathymetry (Figure 16); these additional data are obtained from the DNSC08 model (Andersen et al., 2008) .

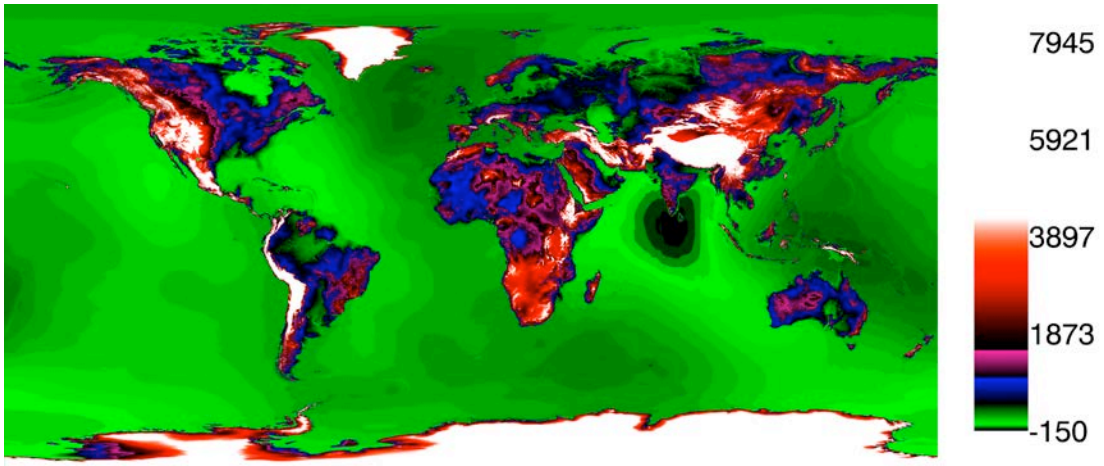

Figure 15 ACE2 dataset fused with sea surface height

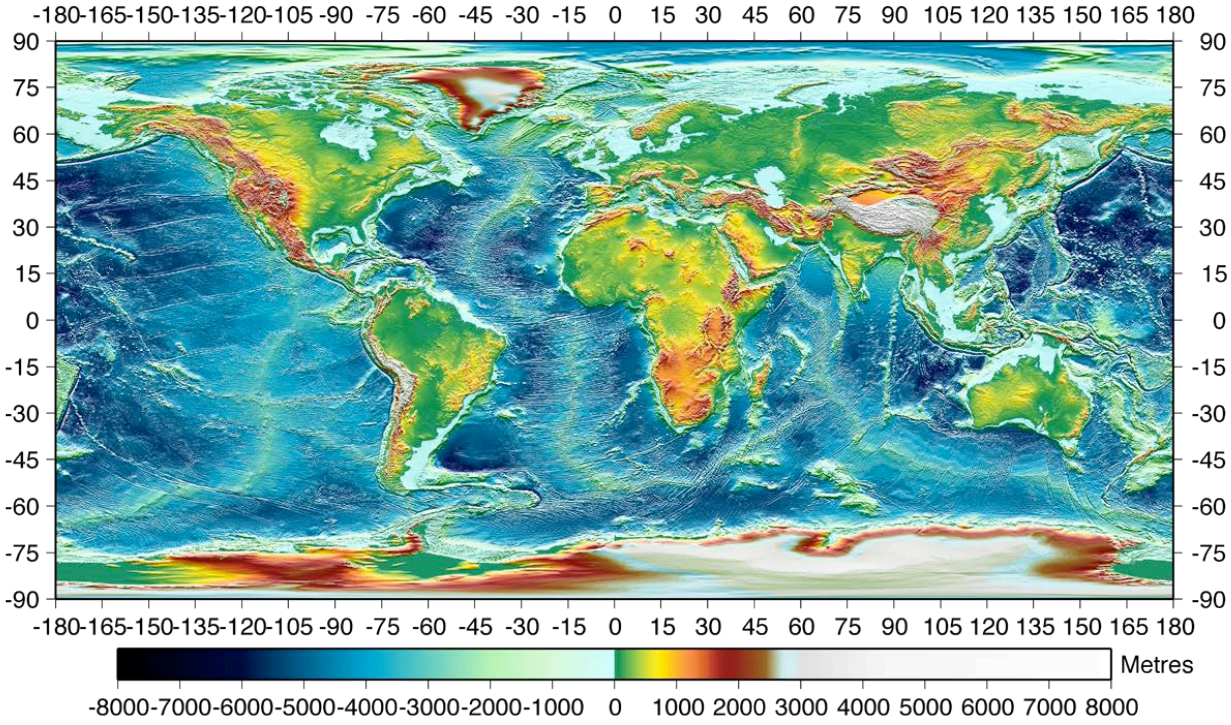

Figure 16 ACE2 dataset fused with bathymetry

5. Discussion

The ACE2 data set has now been released, and is available at a range of spatial scales. This extremely successful development has been made possible by funding from the European Space Agency. Additional information on the ACE2 dataset may be obtained from the website. It is anticipated that further upgrades may be released when additional ground truth data, or spaced-based datasets, become available. In this context, the CryoSat-2 mission is especially relevant, as this will provide enhanced data over much of the Earth's cryosphere.

Acknowledgements

The authors wish to acknowledge ESA, NASA, JPL and CNES for supply of data, and ESA for supporting the ACE2 development.

References

Algiers, J., et al. (1993), TOPEX Ground System Software Interface Specification, (SIS-2) Altimeter Sensor Data Record (SDR) - Alt SDR Data (NASA), March, 1993, JPL D-8591 (Rev. C), TOPEX 633-751-23-001, Rev. C

Andersen et al. The DNSC08 global Mean sea surface and Bathymetry. Presented EGU-2008, Vienna, Austria, April, 2008.

Benveniste, J., et al. (2002), ENVISAT RA-2/MWR Product Handbook, Issue 1.2, PO-TN-ESR-RA-0050, European Space Agency, Frascati, Italy

.
Benada, R. and S. Digby (1997), TOPEX/POSEIDON Altimeter Merged Geophysical Data Record Generation B (NASA/PO.DAAC), JPL PO.DAAC 068.D002, Jet Propulsion Laboratory, Pasadena, CA.

Berry, P.A.M., Hoogerboord, J.E. & Pinnock, R.A., 2000. Identification of common error signatures in global digital elevation models based on satellite altimeter reference data. Phys. Chem. Earth(A), Vol. 25, No. 1, pp 95-99, 2000

Berry, P.A.M., 2000. Topography from land radar altimeter data: Possibilities and restrictions. Phys. Chem. Earth(A), Vol. 25, No. 1, pp 81-88, 2000.

Berry, P.A.M., Garlick, J.D., Smith, R.G., 2007;
Near-global validation of the SRTM DEM using satellite radar altimetry. Remote Sensing of Environment, Vol 106 Issue 1 Pages 17-27, DOI: 10.1016/j.rse.2006.07.011

Brown, C.G., Jr.; Sarabandi, K.; Pierce, L.E., (2005)."Validation of the Shuttle Radar Topography Mission height data," Geoscience and Remote Sensing, IEEE Transactions on , vol.43, no.8pp. 1707- 1715, Aug. 2005

CA. Capp, P. (2001), Altimeter Waveform Product ALT.WAP Compact User Guide, Issue 4.0, PF-UG-NRL AL-0001, Infoterra Ltd., UK.

Denker, S. (2004) Evaluation of SRTM3 and GTOPO30 terrain data in Germany. In: International Association of Geodesy Symposia, Gravity, Geoid and Space Missions , V129, ed C. Jekeli et al., pp 218-223, Springer Verlag, Berlin.

GLOBE Task Team and others (Hastings, David A., Paula K. Dunbar, Gerald M. Elphingstone, Mark Bootz, Hiroshi Murakami, Hiroshi Maruyama, Hiroshi Masaharu, Peter Holland, John Payne, Nevin A. Bryant, Thomas L. Logan, J.-P. Muller, Gunter Schreier, and John S. MacDonald), eds., 1999. The Global Land One-kilometer Base Elevation (GLOBE) Digital Elevation Model, Version 1.0. National Oceanic and Atmospheric Administration, National Geophysical Data Center, 325 Broadway, Boulder, Colorado 80305-3328, U.S.A. Digital data base on the World Wide Web (URL: http://www.ngdc.noaa.gov/mgg/topo/globe.html) and CD-ROMs.

Farr, Tom G., Paul A. Rosen, Edward Caro, Robert Crippen, Riley Duren, Scott Hensley, Michael Kobrick, Mimi Paller, Ernesto Rodriguez, Ladislav Roth, David Seal, Scott Shaffer, Joanne Shimada, Jeffrey Umland, Marian Werner, Michael Oskin, Douglas, Burbank, Douglas Alsdorf, (2007), The Shuttle Radar Topography Mission, Rev. Geophys., 45, RG2004, doi:10.1029/2005RG000183.

Fu, L-L & Cazenave, A (2001). Satellite Altimetry and Earth Sciences, *International Geophysics series Volume 69*, Academic Press.

Hall, O.; Falorni, G.; Bras, R.L., (2005). "Characterization and quantification of data voids in the shuttle Radar topography mission data," Geoscience and Remote Sensing Letters, IEEE , vol.2, no.2pp. 177- 181, April 2005

Hensley, S.; Rosen, P.; Gurrola, E., (2000). "The SRTM topographic mapping processor," Geoscience and Remote Sensing Symposium, 2000. Proceedings. IGARSS 2000. IEEE 2000 International , vol.3, no.pp.1168-1170 vol.3, 2000

Hilton, R. D.; Featherstone, W. E.; Berry, P. A. M.; Johnson, C. P. D.; Kirby, J. F., 2003;. Comparison of digital elevation models over Australia and external validation using ERS-1 satellite radar altimetry. Australian Journal of Earth Sciences, Volume 50, Number 2, April 2003, pp. 157-168(12), DOI:10.1046/j.1440-0952.2003.00982.x

Kellndorfer, J. M., Walker, W. S., Pierce, L. E., Dobson, M. C., Fites, J. A., Hunsaker, C., et al. (2004). Vegetation height estimation from Shuttle Radar Topography Mission and national elevation datasets. Remote Sensing of
Environment, 93, 339–358.

Lemoine, F.G., Kenyon, S.C., Factor, J.K., et al. The Development of the Joint NASA GSFC and the National Imagery and Mapping Agency (NIMA) Geopotential Model EGM96, NASA/TP-1998-206861, 1998.

Scharroo, R., & Visser, P. N. A. M. (1998). Precise orbit determination and gravity field improvement for the ERS satellites. Journal of Geophysical Research, 103(C4), 8113–8127.

Smith, B., & Sandwell, D. (2003). Accuracy and resolution of Shuttle Radar Topography Mission data. Geophysical Research Letters, 30(9), 1467.

USGS website, http://eros.usgs.gov/#/Find_Data/Products_and_Data_Available/gtopo30_info

Zanife, O.Z. J.P. Dumont, J. Stum, T. Guinle (2004), SSALTO Products Specifications - Volume 1: Jason-1 User Products, Issue 3.1, SMM-ST-M-EA-10879-CN, CLS/CNES, Toulouse, France.

APPENDIX A

"ACE2 3 arc second dataset readme"
PRODUCER_FULL_NAME = "Richard Smith "
PRODUCER_INSTITUTE_NAME = "EAPRS Laboratory, De Montfort University, Leicester UK "
PRODUCT_VERSION = 1.31
CREATION_DATE = 2009-11-02

ID = ACE2_3SEC_V1.31

^PER TILE
RESOLUTION = 3 <arc seconds>
DECIMAL_RESOLUTION = 0.05/60
SPATIAL_COVERAGE = 15 * 15 <degrees*degrees>
UNITS = "metres" <m>
ROWS = 18000
COLUMNS = 18000
TOTAL_NUMBER = 324000000
BYTE_ORDER = "LITTLE ENDIAN"
DATA_TYPE = float
SAMPLE_BITS = 32 <bit>
BANDS = 1
DATA_DIRECTION = "EAST"

TILE_DESCRIPTION = "Data in a row major form (i.e. row 1 then row 2)
Data run North to South (i.e. row 1 = furthest North, row 18000 = furthest South)
Co-ordiante in the filename refers to the South West (lower left) edge of the tile i.e. the lower left corner of the lowest left pixel"

^GLOBAL INFO
OCEAN_VALUE = -500
VOID_VALUE = -32768
REFERENCE_ELLIPSOID = "WGS84"
GEOID_MODEL = "EGM96"
PROJECTION = "Simple Cylindrical"
CENTRE_LATITUDE = 0
CENTRE_LONGITUDE = 0
MAX_LAT = 90
MIN_LAT = -90
MAX_LON = 180
MIN_LON = -180
CO-ORDINATE_SYSTEM = "GEODETIC"